CHAPTER 3

ENERGY AND EXERGY COMPARISON OF ORGANIC PCMS BASED TES SYSTEM INTEGRATED WITH IC ENGINE

The energy and exergy analysis comparisons of the TES system integrated with IC engine exhaust by the variation of mass fraction from 0.1kg to 0.4kg in organic PCMs (capric acid, lauric acid, paraffin wax, and stearic acid) have been discussed in this chapter. This chapter is broadly divided into three sections. The first section evaluated a description of experimental components, procedures, and uncertainty results. Data reduction for the energy and exergy analysis of the TES system integrated with engine exhaust was considered in the second section. However, the last section of this chapter studied the results and discussions of the parameters, i.e., thermal performance, charging time, discharging time, etc.

3.1. Experimental Analysis

3.1.1. Description of the experimental setup

The experimental setup has been classified into five components: an IC Engine, shell and tube heat exchanger, heat transfer fluid (HTF) system, concentric tube type thermal energy storage (TES) system, and temperature sensor devices. The descriptions of types of equipment are given below:

3.1.1.1. Internal Combustion Engine

The experiment was conducted on the four strokes, four-cylinder diesel engine test rig with a water brake dynamometer. Fig 3.1 shows the engine test rig on which experiments were conducted. It consists of four strokes, a four-cylinder diesel engine, hydraulic dynamometer, temperature sensors, fuel tank, fuel flow meter, crank angle sensor, air box, and heavy-duty battery. The TATA Indigo model was used as a diesel engine. The specification of the diesel engine is presented in Table 3.1. A dynamometer is used to measure the load on the engine. The dynamometer absorbs the power generated by the primary mover. The dynamometer's absorbed power must be dispersed into the atmosphere or transmitted to cooling water.

The thermocouple is the most efficient way to monitor the temperature. The type of thermocouple employed in this investigation is chromel-alumel (K-type). The chromel-alumel thermocouple has a temperature range of -17.78^{o}C to 1260^{o}C degrees. The thermocouples are mounted to measure the temperature at the inlet and outlet of coolant, outlet of exhaust gas, and the inlet air temperature after and before turbocharged. Two fuel tanks are included, one with a greater diameter and the other with a smaller diameter. Both tanks are connected at the bottom by a glass tube that runs parallel. The glass tube has a diameter of 6mm, whereas the gasoline tank has a diameter of 72 mm. Flow meters are used to measure the discharge of fuel. Also, on a diesel engine, an orifice meter is used to measure the mass flow rate of the coolant flow. A crank angle sensor is an electrical device used for monitors the position or rotational speed of the crankshaft of an engine.

Furthermore, a battery is attached, having 12 volts and 80 Ampere-hour capacity. However, a 7kg load was applied to the engine through the water to the dynamometer.

Based on the 7kg load and with a particular dynamometer shaft rotation of 1500 rpm, the brake power of the engine has been calculated. This load was indicated on the dynamometer balance. The temperature of exhaust gases produced at the outlet was favourable and suiTable , and less vibration for the engine load of 7kg with 1500rpm.

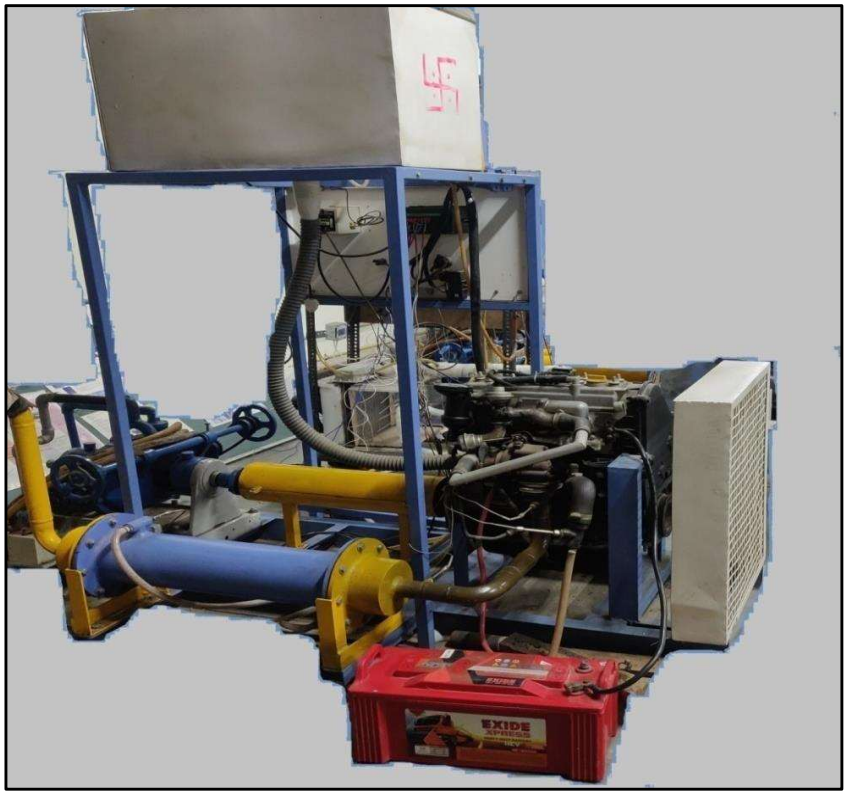

Fig.3.1. The Engine test rig

Table 3.1: Specification of Diesel Engine

Fuel type	Diesel	**Bore**	75mm
Model	TATA Indigo	**Stroke length**	79mm
Maximum power	71 Bhp @ 4000rpm	**Compression ratio**	21:1
Maximum Torque	140Nm @1800 rpm	**Cooling**	Water-cooled
No. of Cylinder	Four	**Cubic centimeter**	1396 CC

3.1.1.2 . TES system filled with Phase change materials (PCMs)

Thermal energy storage (TES) is a method of storing thermal energy by heating or cooling a storage medium that can then be used for subsequent heating, cooling, or power generation. The present research uses the concentric cylindrical tube type TES system, as shown in Fig. 3.2. The TES system is fabricated with stainless steel. The specification of the TES system is given in Table 3.2. The heat transfer fluid flows in the inner tube, and phase change material fills the outer tube.

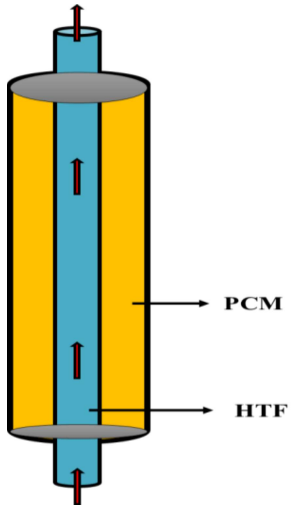

Fig.3.2. The concentric cylindrical type TES system

Table 3.2: Specification of Concentric cylindrical TES system

The outer diameter of the outer tube (D_o)	63.50mm	**Length of TES system (l)**	300mm
The outer diameter of the inner tube (d_o)	25.40mm	**Material of the outer tube**	Stainless steel
Wall thickness of outer tube (t_{ws})	1.10mm	**Material of the inner tube**	Stainless steel
Wall thickness of the inner tube (t_{wt})	0.84mm		

The phase change materials supplied in the TES system have been directly purchased from different industries. CA (pure), LA (pure), and SA (pure) PCMs have been purchased from Sisco research laboratories private limited. PW (with≤ 0.05% sulfated ash) was purchased from Merck life science Private Limited. The sample of PCMs is shown in Fig.3.3.The specific heat capacity of capric acid (CA), lauric acid (LA), paraffin wax (PW) and stearic acid (SA) are 2.43-2.92kJ/kg-K, 1.98-2.35 kJ/kg-K, 2.24-3.21 kJ/kg-K, 1.82-2.14 kJ/kg-K respectively. Howerver, the thermal conductivity of capric acid (CA), lauric acid (LA), paraffin wax (PW) and stearic acid (SA) are 0.12-0.178W/m-K, 0.126-0.174W/m-K, 0.09-0.148W/m-K and 0.138-0.15W/m-K,respectively.

CA **LA** **PW** **SA**

Fig.3.3. Samples of CA, LA, PW, and SA PCMs

3.1.1.3 . The heat exchanger (HEX)

A U tube-type shell heat exchanger was used in the experiment setup, as shown in Fig. 3.4. The U tube heat exchanger is a type of tube and shell heat exchanger used in the petroleum and chemical industries. The tube box, shell, and tube buddle are the primary components of a U tube heat exchanger. The tube bundle in this heat exchanger is U-shaped, as the name implies. The tubes begin from the bottom of the tube sheet, form a U, and then return to the tube sheet's top. Table 3.3 shows the specification of the heat exchanger. The theoretical and actual effectiveness was obtained within 0.60–0.72 and 0.58–0.65, respectively.

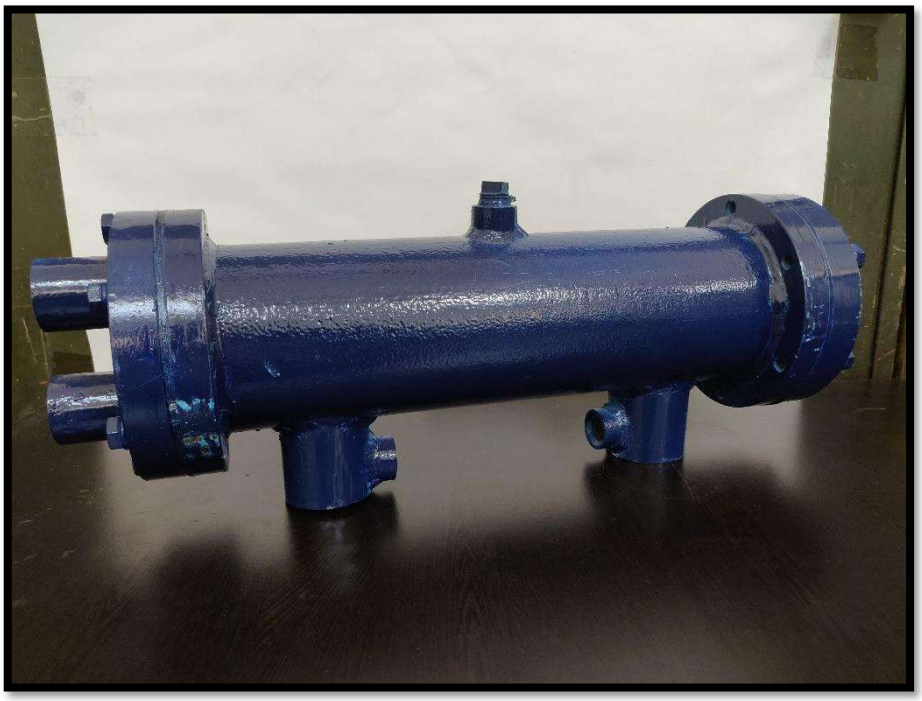

Fig.3.4: The shell and tube heat exchanger

Table 3.3: Specification of shell and tube heat exchanger

Total length	500mm	**Tube pitch**	14.292mm
Shell outer diameter	100mm	**Transverse tube pitch**	14.292mm
Thickness of shell	5mm	**Longitudinal tube pitch**	14.292mm
Length of shell	400mm	**Central baffle spacing**	90mm
No. of Baffles used	2	**Inlet baffle spacing**	90mm
The thickness of the tube sheet	20mm	**Outlet baffle spacing**	90mm
Thickness of baffles	3mm	**Baffle cut spacing**	25mm
The thickness of Tie Rod	6mm	**Material of shell**	MS
Tube outer diameter	9.528mm	**Material of tube**	Copper
Tube inner diameter	9.2446mm	**Material of tube sheet**	MS
No. of tubes	12	**Material of the channel flange**	MS
Length of tube	400mm	**Material of baffles**	MS
No. of passes	2	**Material of tie rod**	MS

3.1.1.4. Heat transfer fluid (HTF) system

In a heat transfer fluid system, three major components are i.e., the HTF Storage tank, magnetic pump, and rotameter, as shown in Figs. 3.5-3.7, respectively. The HTF storage tank is stainless steel, having 10 liters capacity. The HTF was circulated with the help of a magnetic pump and purchased from Promivac Engineers (India). The magnetic pump operates on a very basic principle. Because the magnets in the outer and inner magnet rings are attracted, the outer and inner rings revolve at the same speed as the electric motor, turning the impeller and allowing liquid to be pumped. The maximum head and capacity of the attached magnetic pump are 5 meters and 1800 LPH, respectively. The pump worked on a single phase 220/240 Volts AC supply with 0.32A, 70W. It runs at a constant RPM of 2800 with a 50 Hz frequency.

Fig.3.5. The HTF Storage tank

Fig.3.6. The magnetic drive pump

Fig.3.7. The rotameter

The rotameter was used to measure the flow rate of HTF and manufactured by Star Flow (India). A rotameter is a tapered tube, usually made of glass, with a 'float' within that is pushed up by the flow's drag force and dragged down by gravity. A rotameter does not require any external energy or fuel. Furthermore, because it is made of low-cost components and transparent glass, it is cheap in cost and highly resistant to heat stress and chemical action. In the following experiments, the maximum flow rate capacity of the rotameter is 5 LPM.

3.1.1.5. Temperature sensor devices

However, the PT100 type thermocouple was used in the experiment having a temperature range -200^{o}C to 850^{o}C, as shown in Fig. 3.8. The sensor type, Pt100, denotes two crucial characteristics of the sensor. The first portion, Pt, is the chemical symbol for Platinum, indicating that the sensor is made of this metal. The second portion, 100, refers

to the device's resistance at 0°C. In this situation, the number is 100Ω. These thermocouples were calibrated with the reference thermocouple (model number WL202 manufactured by Osawa Industrial Products Pvt. Ltd.) from 0°C to 100°C.

Fig.3.8. PT100 type thermocouple

Fig.3.9. Digital data logger

The thermocouples were coupled with a sixteen-channel digital data logger, which displayed temperature and recorded temperature values. Digital data loggers are shown in Fig. 3.9. A temperature data logger, often known as a temperature monitor, is a porTable measuring device that can independently record temperature during a specified period. After it has been recorded, the digital material may be accessed, examined, and analyzed. The attached digital data logger was manufactured by the Countronics industry, Ghaziabad, India. Table 3.3 shows the specification of the digital data logger.

Table 3.4: Specification of digital data logger

Parameters	Specification
Display	4×20 line 0.3" character height alphanumeric LCD module display
Sensor	J/K/R Thermocouples and 3 wire PT100 sensor user selecTable
Range	J-T/C : 0 to 750˚C K-T/C : 0 to 1250˚C R-T/C : 0 to 1700˚C PT100: -100.0 to +600.0˚C
Resolution	1˚C for thermocouples and 0.1˚C for PT100
Channels	Maximum 16
Scanning Rate	User setTable from 1-99seconds
Digital Offset	User setTable individually for each channel
Logging Rate	1 second to 99Mins59seconds
Data Logging	Directly create a .csv file on the Pen Drive (compatible with Excel) giving a tabular format value of Date, Time, and selected channels
Real Time Clock	AdjusTable Calendar (Month/Date) and Time (Hrs: Mins)
Accuracy	±1˚C ± 1 Least Significant Digit for Thermocouples ±0.1˚C ± 1 Least Significant Digit for PT100
Power Supply	230V AC ± 15% at 50/60Hz
Mounting Type	Panel Type
Front Facia	96mm x 192mm

3.2. Uncertainties analysis

The uncertainties analysis for the parameters prediction was calculated using (Holman et al., 2001) Eqs.3.1 and 3.2. Where P is the measured value dependent on unrelated measured parameters Q_1, Q_2, Q_3.....Q_n and R_1, R_2, R_3…… R_n is the uncertainties in the independent variables.

$$P = P(Q_1^{R_1}, Q_2^{R_2}, Q_3^{R_3} \dots\dots\dots Q_n^{R_n}) \quad (3.1)$$

Then the uncertainties (U_S) can be expressed by: (Shaikh et al., 2008)

$$U_S = \sqrt{[\left(\frac{\partial P}{\partial Q_1} R_1\right)^2 + \left(\frac{\partial P}{\partial Q_2} R_2\right)^2 + \left(\frac{\partial P}{\partial Q_3} R_3\right)^2 + \quad \dots\dots\dots\dots\dots\dots \left(\frac{\partial P}{\partial Q_n} R_n\right)^2]} \quad (3.2)$$

Table 3.4 and Table 3.5 show the accuracy of instruments and maximum uncertainties of parameters, respectively.

Table 3.5: Accuracy of Instruments

Instrument	Value
Stopwatch	±0.2%
Digital weighing machine	±0.4%
Measuring flask	±0.3%
Thermocouple	±0.5°C

Table 3.6: Calculated maximum uncertainties

Parameters	Uncertainties
Fuel consumption volume	±0.2
Time taken	±0.3
Dynamometer load	±0.1
Mass of fuel	±0.5
Volume of fuel	±0.6
Temperature	±0.2

3.3. Description and methodology for energy and exergy comparison of organic PCMs

The following sections cover the TES system's experimental methodologies, geometry, and boundary conditions. In addition, the equations for comparing organic PCMs-based TES systems in terms of energy and exergy have been presented.

3.3.1 Description and methodology of the physical model of TES system integrated IC engine

The experiments were conducted at a 7kg load and 1500 engine rpm. A dynamometer was used for loading the test engine, and the fuel consumption was measured using the burette method for an equal interval of time for the consumption of 5ml of fuel. The TES system was filled with organic PCMs such as capric acid, lauric acid, paraffin wax, and stearic acid PCMs of mass fractions from 0.1kg to 0.4kg. The TES system is charged with the help of water as HTF, which circulated from the HTF tank through a magnetic drive pump to a shell-and-tube-type heat exchanger at a constant flow

rate of 2 LPM. The heat exchanger (HEX) consists of tubes through which the hot water passes from the engine exhaust to extract waste heat from the exhaust gas. The energy is stored in the TES system in the form of heat increases the temperature in the TES system. The rotameter was used to measure the flow rate of HTF, and for maintaining a constant flow rate, a bypass valve and dimmer were used.

Furthermore, the thermocouples were placed to measure the temperature at the various locations of the experimental setup. At considered engine load and rpm, an optimum temperature of 180°C and 110°C was obtained at exhaust gases inlet and outlet ports. The temperature of HTF reached 80°C by receiving heat from exhaust gases. The HTF storage tank, pipeline, and TES system were well insulated with plaster of Paris and rubber sheets, respectively, to enhance heat transfer. The schematic diagram of an experimental setup is shown in Fig. 3.10. Also, Fig. 3.11 shows the flowchart of the experimental procedure. The engine performance test was conducted with and without the heat exchanger. The heated water is directed to the PCM's thermal energy storage (TES) system, which heats it. Temperature readings were taken at a regular interval of 10min throughout the charging period for various mass fractions of organic PCMs. Each experiment has been repeated six times, and on the base, an error bar has been induced in the obtained results.

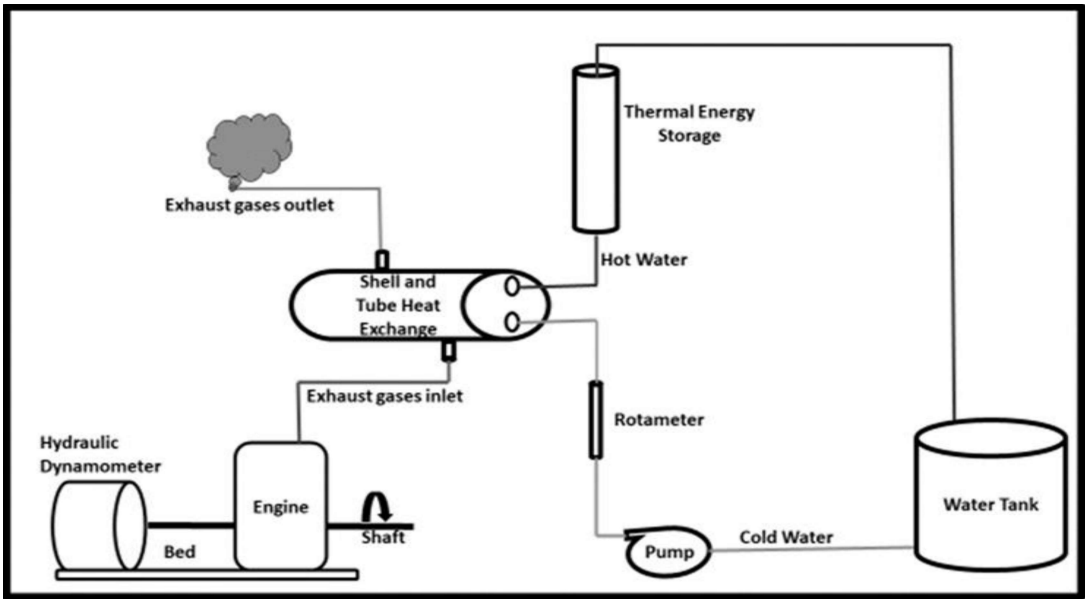

Fig.3.10. The schematic diagram of an experimental setup

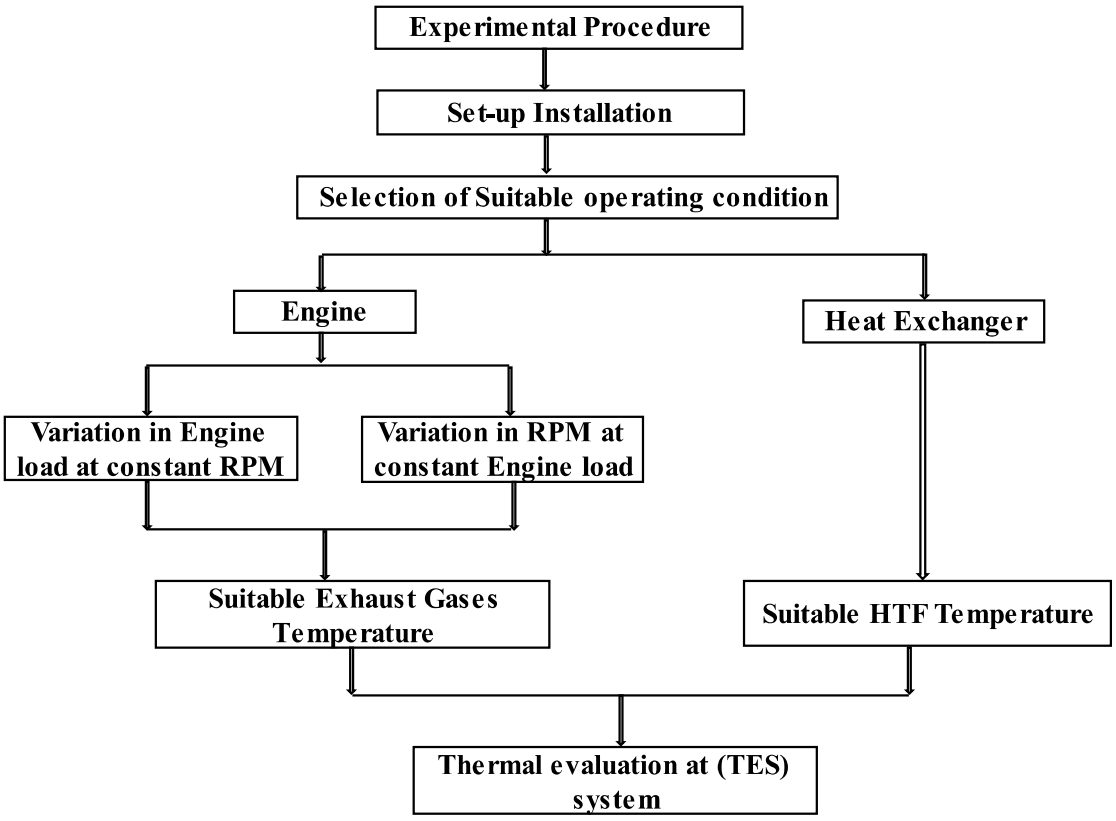

Fig.3.11. Flow chart of Experimental procedure

3.3.2 Geometry and Boundary conditions of the TES system

The vertical concentric tube type TES system has been used for energy and exergy analysis. Two stainless steel tubes, 63.5mm and 25.4mm in diameter and 300mm in length, were used to fabricate the TES system. Heat was transferred from HTF to PCM in a radial direction. The heat transfer modes of conduction and convection have both been observed. Conduction from HTF to tube and tube to PCM occurs, whereas convection occurs in the liquid phase of PCM. Fig. 3.12 shows the schematic diagram of the problem under consideration.

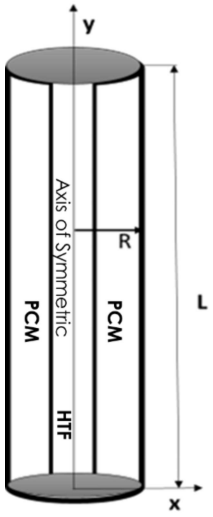

Fig.3.12. Schematic diagram of the problem under consideration

The following initial and boundary conditions have been considered:

Initial condition(t=0): T(x,y,0) =Ta, u=v=0

The bottom part of the TES system (t >1): $\frac{\partial T(x,0,t)}{\partial y} = 0$, u=v=0

Lateral wall of the TES system (t >1): T(R,y,t) = Tpcm, u=v=0

Upper part of the TES system(t>1): T(x,L,t) = Tpcm, u=v=0

3.3.3. Equation used in Energy analysis of TES system(Gopal et al., 2010),

Engine output power (W_d),

$$W_d = 0.746 \times bhp \tag{3.3}$$

Mass rate of fuel (m_f),

$$m_f = s.f.c \times W_d \tag{3.4}$$

Fuel energy (E_f),

$$E_f = m_f \times CV \tag{3.5}$$

The energy carried by exhaust gases without a heat exchanger (E_{ex}),

$$E_{ex} = m_{ex} \times c_{pex} \times (T_{e1} - T_o) \tag{3.6}$$

$$where\ m_{ex} = m_f + m_a$$

The energy carried by coolant (E_c),

$$E_c = m_c \times c_{pc} \times (T_{c2} - T_{c1}) \tag{3.7}$$

where, $m_c = \rho_c \times v_c$

The energy lost due to accounted factors ($E_{unaccount}$),

$$E_{unaccount} = E_f - (E_{ex} + E_c + W_d) \tag{3.8}$$

Energy carried by exhaust gases with heat exchanger (E_{ehx}),

$$E_{ehx} = m_{ehx} \times c_{pex} \times (T_{e1} - T_{e2}) \tag{3.9}$$

Charging rate (E_{ch}), $E_{ch} = \frac{E_w + E_p}{t}$ (3.10)

where, $E_w = m_w \times c_{pw} \times (T_{w2} - T_{w1})$ and

$$E_p = m_p \times c_{pp} \times (T_{p2} - T_{p1}) + m_p \times LH$$

Charging efficiency of the system (η_{ch}),

$$\eta_{ch} = \frac{E_{ch}}{E_{ehx}} \tag{3.11}$$

Total useful energy (E_t),

$$E_t = W_d + E_{ch} \tag{3.12}$$

Energy efficiency of the diesel engine (η_d),

$$\eta_d = \frac{W_d}{E_f} \tag{3.13}$$

Energy efficiency of the integrated system (η_i),

$$\eta_i = \frac{E_t}{E_f} \tag{3.14}$$

Energy saved (η_s),

$$\eta_s = \frac{E_{ch}}{E_f} \tag{3.15}$$

3.3.4. Equation used in Exergy analysis of TES system (Gopal et al., 2010);

Chemical availability of a fuel (A_f),

$$A_f = 1.04 \times m_f \times CV \tag{3.16}$$

Exergy lost in exhaust gas without heat exchanger (A_{ex}),

$$A_{ex} = m_{ex} \times C_{pex} \times [(T_{e1} - T_o) - T_o \times ln\frac{T_o}{T_{e1}}] \tag{3.17}$$

Exergy lost by coolant (A_c),

$$A_c = m_c \times C_{pc} \times [(T_{c2} - T_{c1}) - T_o \times ln\frac{T_{c2}}{T_{c1}}] \quad (3.18)$$

Exergy lost due to unaccounted factors ($A_{unaccounted}$),

$$A_{unaccounted} = A_f - [A_{ex} + A_c + W_d] \quad (3.19)$$

Exergy is lost in the exhaust gas when the heat exchanger is present (A_{ehx}),

$$A_{ehx} = m_{ex} \times C_{pex} \times [(T_{e1} - T_{e2}) - T_o \times ln\frac{T_{e1}}{T_{e2}}] \quad (3.20)$$

Charging rate of integrated system (A_{ch}),

$$A_{ch} = \frac{A_{st1}+A_{st2}+A_{st3}}{t} \quad (3.21)$$

where, $A_{st1} = m_w \times C_{pw} \times [(T_{w1} - T_{w2}) - T_o \times ln\frac{T_{w1}}{T_{w2}}]$

$$A_{st2} = m_p \times C_{pp} \times \left[(T_{p1} - T_{p2}) - T_o \times ln\frac{T_{p1}}{T_{p2}}\right]$$

$$A_{st3} = m_p(LH - T_o \times \frac{LH}{T_{pcm}})$$

Total useful exergy (A_t); $A_t = W_d + A_{st}$ (3.22)

Exergy efficiency of system (ψ_d),

$$\psi_d = \frac{W_d}{A_f} \quad (3.23)$$

Exergy efficiency of an integrated system (ψ_i),

$$\psi_i = \frac{A_t}{A_f} \quad (3.24)$$

The exergy efficiency of charging (ψ_{ch}),

$$\psi_{ch} = \frac{A_{st}}{A_{ehx}} \tag{3.25}$$

Exergy saved from the exhaust (ψ_s),

$$\psi_s = \frac{A_{st}}{A_f} \tag{3.26}$$

3.4. Data Reduction

3.4.1. Charging Time of TES System

The time-temperature curve during charging of capric acid, lauric acid, paraffin wax, and stearic acid PCMs with the mass fractions within the range of 0.1- 0.4 kg is shown in Figs. 3.13 –3.16. The charging time of PCM with various mass fractions is taken at a regular interval of 10 min. Results revealed that the charging time of capric acid, lauric acid, paraffin wax, and stearic acid PCMs are increased by 51.35%, 53.85%, 129.16%, and 88.89%, respectively, for a mass variation from 0.1kg to 0.4kg. However, it has been observed that the TES system with the 0.4 kg mass of paraffin wax required 46.42%, 83.33%, and 29.41% higher than capric acid, lauric acid, and stearic acid, respectively. The charging time in the case of paraffin wax was higher than the capric acid, lauric acid, and stearic acid PCMs due to high heat of fusion and less thermal conductivity than capric acid, lauric acid, and stearic acid PCMs.

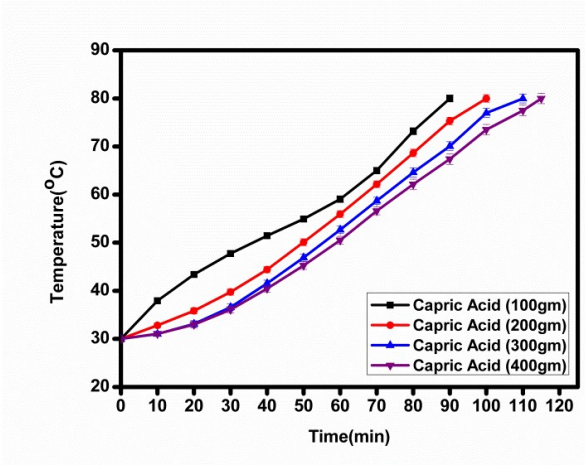

Fig.3.13. Charging time of CA PCM with the mass fraction

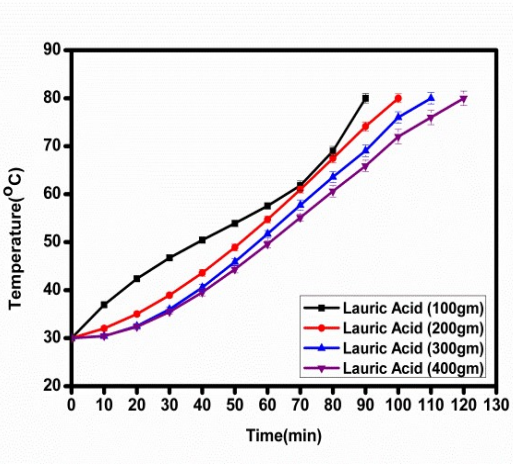

Fig.3.14. Charging time of LA PCM with the mass fraction

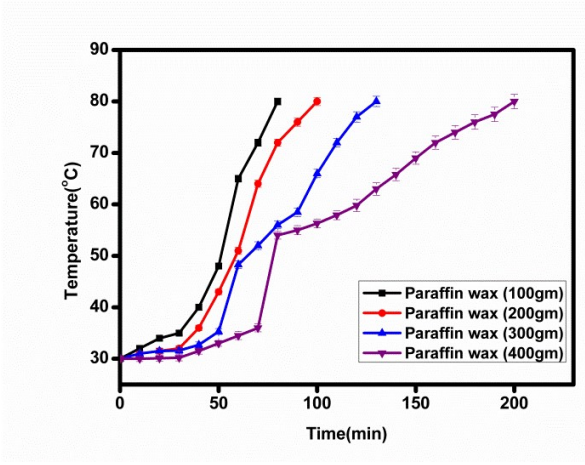

Fig.3.15. Charging time of PW PCM with the mass fraction

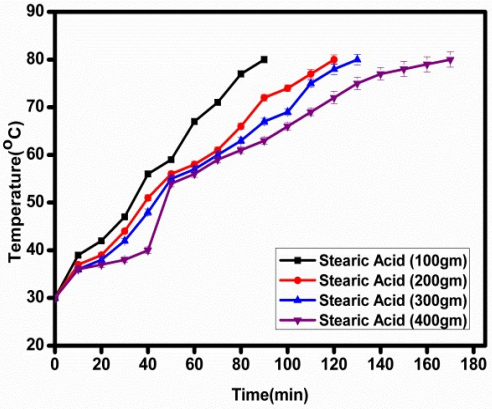

Fig.3.16. Charging time of SA PCM with the mass fraction

3.4.2. Discharging Time of TES System

Time-Temperature curve during discharging capric acid, lauric acid, paraffin wax, and stearic acid PCMs with the various mass fractions of PCMs, has been shown in Figs. 3.17–3.20. For the mass of 0.4 kg, capric acid, lauric acid, paraffin wax, and stearic acid have 77.38%, 70.21%, 38.40%, and 40.35%, respectively, temperature differences within a time interval range of 0–100min. The decrement in temperature of capric acid PCM

shows a faster rate than lauric acid, paraffin wax, and stearic acid PCMs due to variation in melting temperature, specific heat capacity, and specific enthalpy. It may happen because capric acid PCM has moderate thermal conductivity than lauric acid, paraffin wax, and stearic acid PCMs. But, in the case of stearic acid PCM, the solidification point is at 57°C, and the constant temperature line has been observed. Furthermore, the variation in error value for charging and discharging temperature was determined to be 0.6 - 1°C.

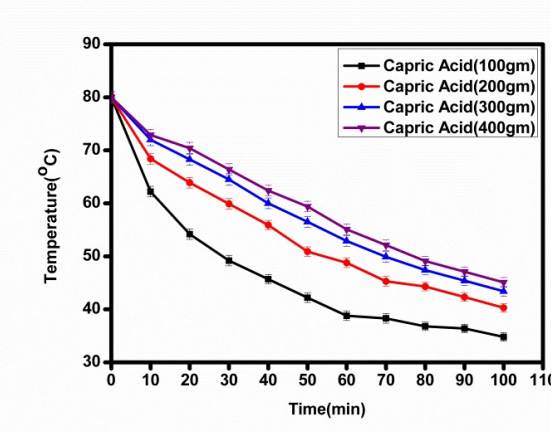

Fig.3.17. Discharging time of CA PCM with the mass fraction

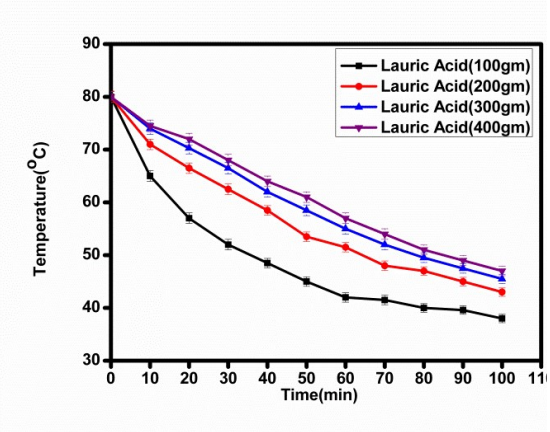

Fig.3.18. Discharging time of LA PCM with the mass fraction

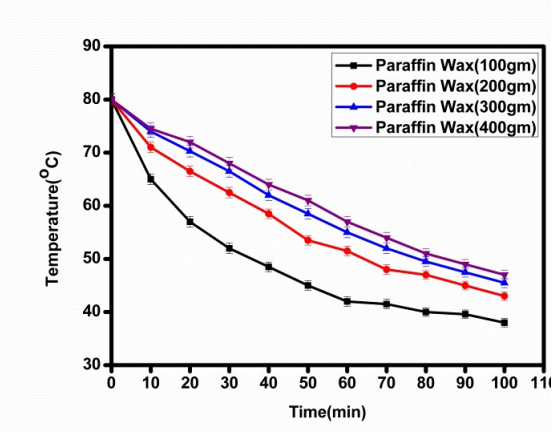

Fig.3.19. Discharging time of PW PCM with the mass fraction

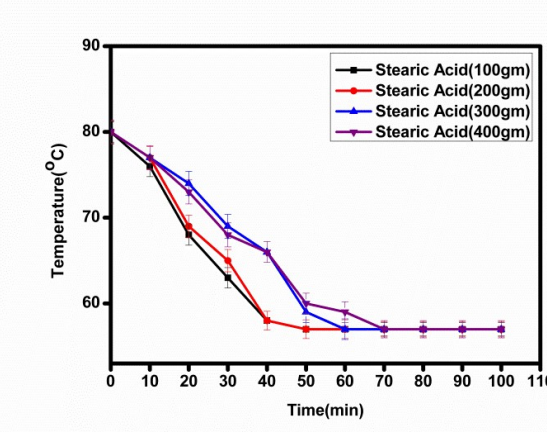

Fig.3.20. Discharging time of SA PCM with the mass fraction

3.4.3. Energy Analysis of TES System

This section has done energy analysis of organic PCMs-based TES system coupled with IC engine. As the mass fraction variation of PCMs from 0.1kg to 0.4 kg, the interpretation of the energy storage medium has been shown in Fig. 3.21. Results revealed that the storage medium energy of capric acid, lauric acid, and stearic acid-based TES system was increased by 122.8%, 5.66%, and 99.06%, respectively. But in the case of the paraffin wax PCM-based TES system, the energy of the storage medium was decreased by 52.8%. Fig.3.22 shows the energy efficiency of charging for the 0.1- 0.4kg mass fractions of PCMs. Results revealed that the energy efficiency of charging capric acid, lauric acid, and stearic acid-based TES systems increased by 122.85%, 5.63%, and 99.17%, respectively, for the mass fraction variation of 0.1-0.4kg. But, it was reduced by 68.87% in the paraffin wax PCM-based TES system for the mass fraction variation of 0.1-0.4kg.

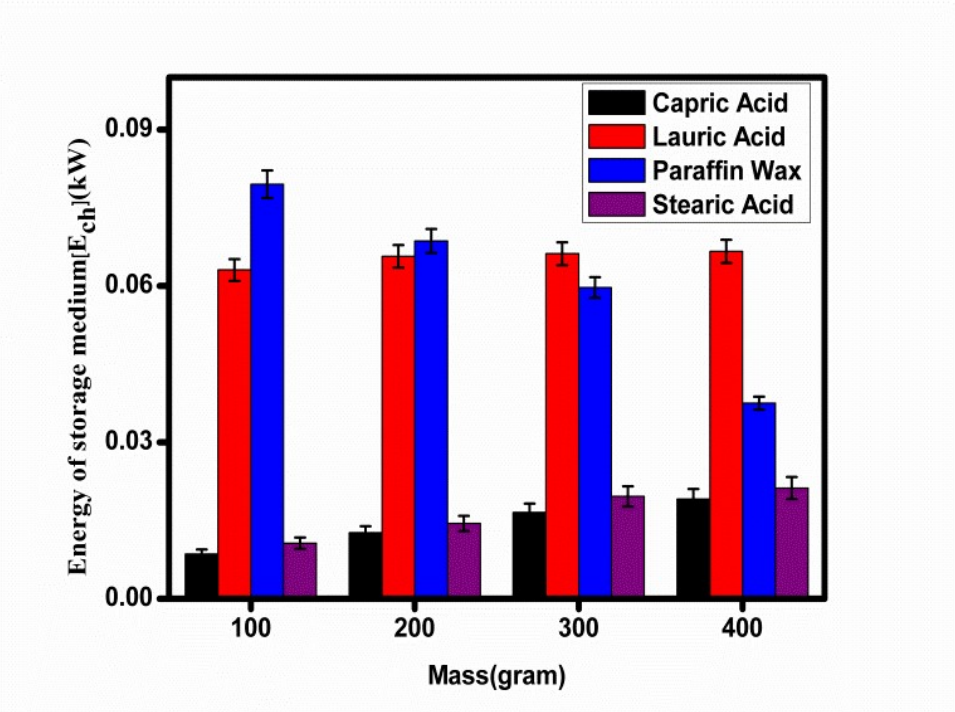

Fig.3.21. Variation in the energy of storage medium

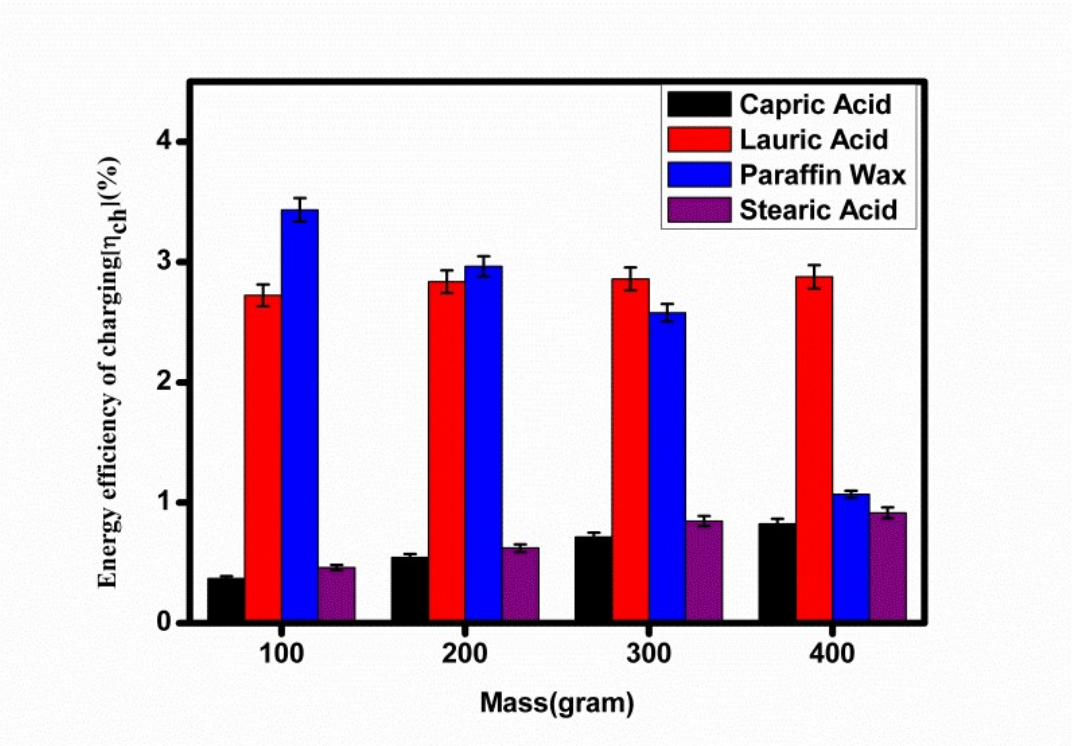

Fig.3.22. Variation in the energy efficiency of charging

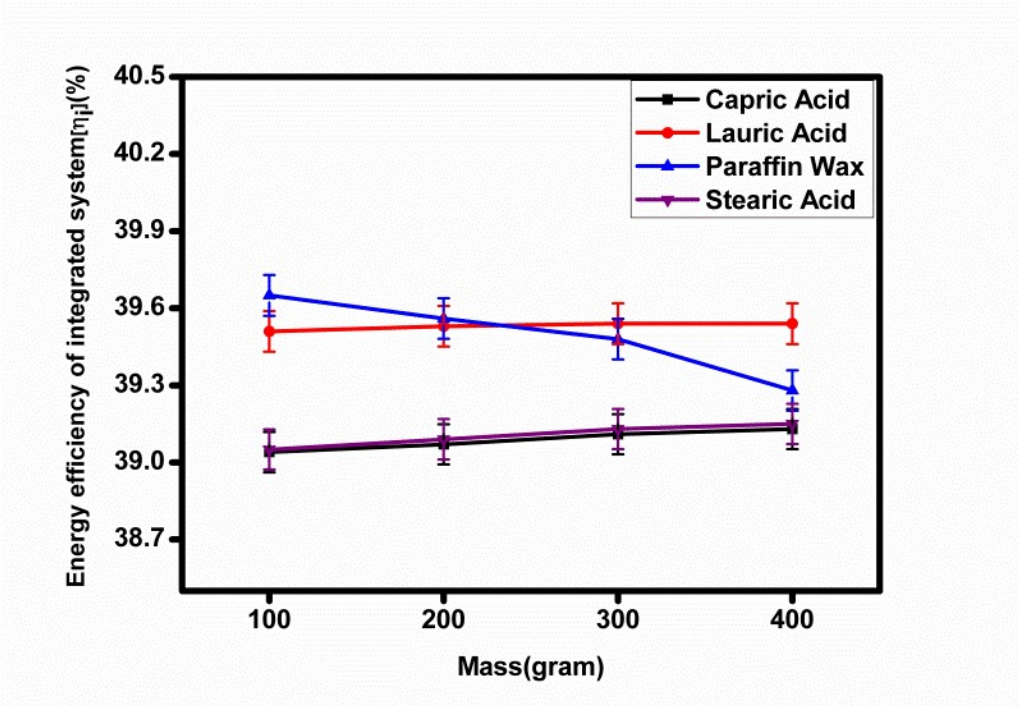

Fig.3.23. Variation in the energy efficiency of the integrated system

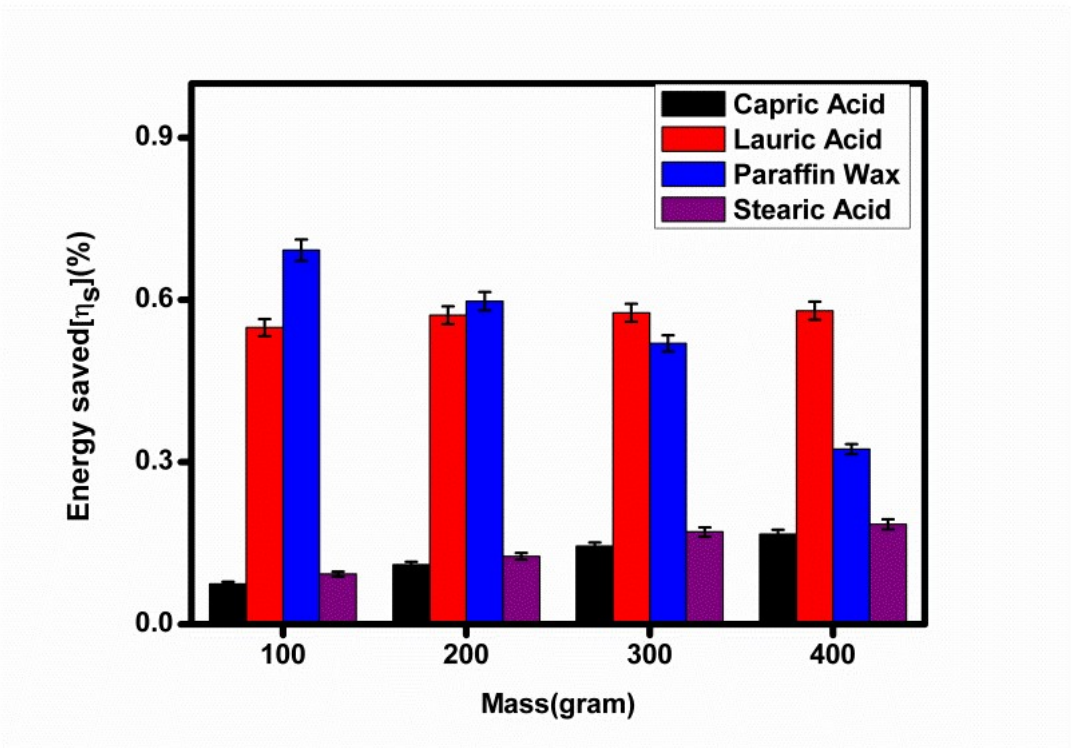

Fig.3.24. Variation in the energy saved

However, Fig. 3.23 shows the variation in the energy efficiency of the integrated system for the various mass fraction variation of 0.1-0.4kg. It has been observed that the energy efficiency of the integrated system of capric acid, lauric acid, and stearic acid-based TES system was increased by 0.23%, 0.076%, and 0.26%, respectively, for the mass fraction variation of 0.1-0.4kg. But in the case of the paraffin wax PCM-based TES system, it was reduced by 0.93% for the mass fraction variation of 0.1-0.4kg. For the mass fraction variation of PCMs from 0.1kg to 0.4kg, the interpretation of energy saved has been shown in Fig.3.24. It has been found that the energy saving of capric acid, lauric acid, and stearic acid-based TES systems was increased by 122.84%, 5.66%, and 99.13%, respectively. But in the case of the paraffin wax PCM-based TES system, energy saved was decreased by 53.19% for the mass fraction variation of 0.1-0.4kg. However, the energy analysis of the TES system with a mass of 0.3kg lauric acid PCM has optimum

results at engine 7kg load at 1500 RPM. It may be because the charging time is the primary factor that affects the energy analysis of organic PCMs-based TES systems.

3.4.4. Exergy Analysis of TES System:

Exergy analysis of organic PCMs-based TES system with IC engine has been performed. The variation of exergy storage medium has been exhibited in Fig. 3.25, as the mass fraction of PCMs varies from 0.1kg to 0.4kg. The exergy of storage medium capric acid, lauric acid, and stearic acid-based TES systems was raised by 74.53 %, 3%, and 108%, respectively. The exergy of the storage medium was reduced by 53.36 % in the paraffin wax PCM-based TES system. The exergy efficiency of charging PCM mass fractions 0.1kg-0.4kg is shown in Fig. 3.26. For the mass fraction variation of 0.1-0.4kg, the exergy efficiency of charging capric acid, lauric acid, and stearic acid-based TES systems increased by 74.48%, 2.9%, and 108%, respectively. However, the mass fraction variation of 0.1-0.4kg was reduced by 53.36 % using a paraffin wax PCM-based TES system. The variation in exergy efficiency of the integrated system for various mass fraction variations of 0.1-0.4kg is seen in Fig. 3.27. The exergy efficiency of the integrated system is the ratio of total useful exergy to chemical availability. For the mass fraction variation of 0.1-0.4kg, the exergy efficiency of the integrated system of stearic acid-based TES system increased by 0.026%. However, the mass fraction variation of 0.1-0.4kg was reduced by 0.08% using a paraffin wax PCM-based TES system with a mass fraction increase of 0.1 to 0.4kg; it was revealed that the integrated system of lauric acid has a higher total exergy efficiency than stearic acid and capric acid PCMs. This is because lauric acid has greater total exergy of used from fuel. Total exergy used from fuel input for paraffin wax, stearic acid PCM, and capric acid decreases with mass fraction change from 0.1 to 0.4kg because of increased charging time and low specific heat

capacity. With a mass variation of 0.1 to 0.4kg, total exergy consumed from fuel input directly influenced the exergy efficiency of the integrated system, resulting in exergy improved efficiency of lauric acid.

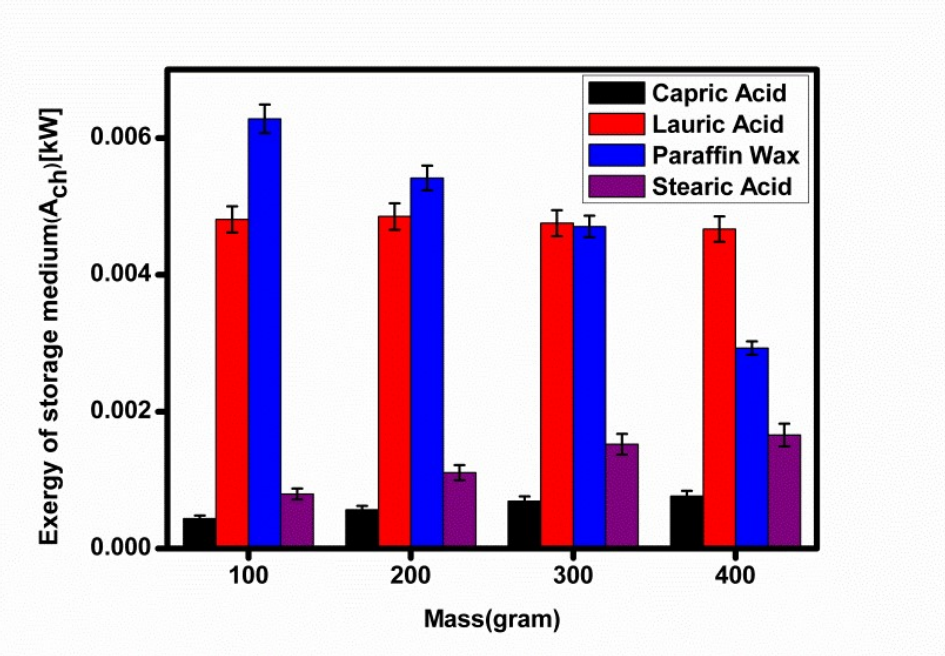

Fig.3.25. Variation in exergy of storage medium

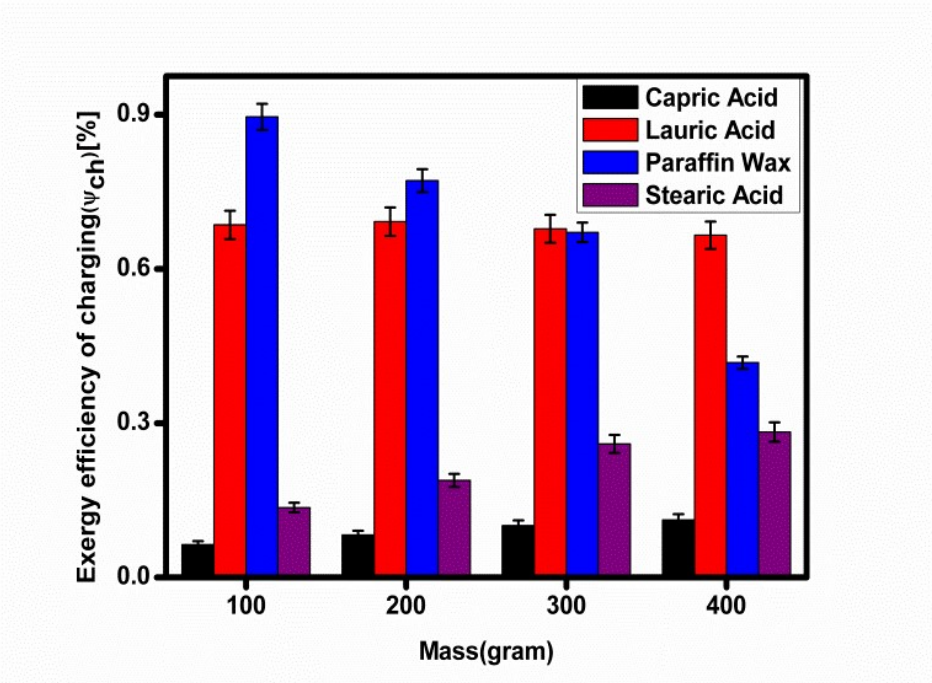

Fig.3.26. Variation in the exergy efficiency of charging

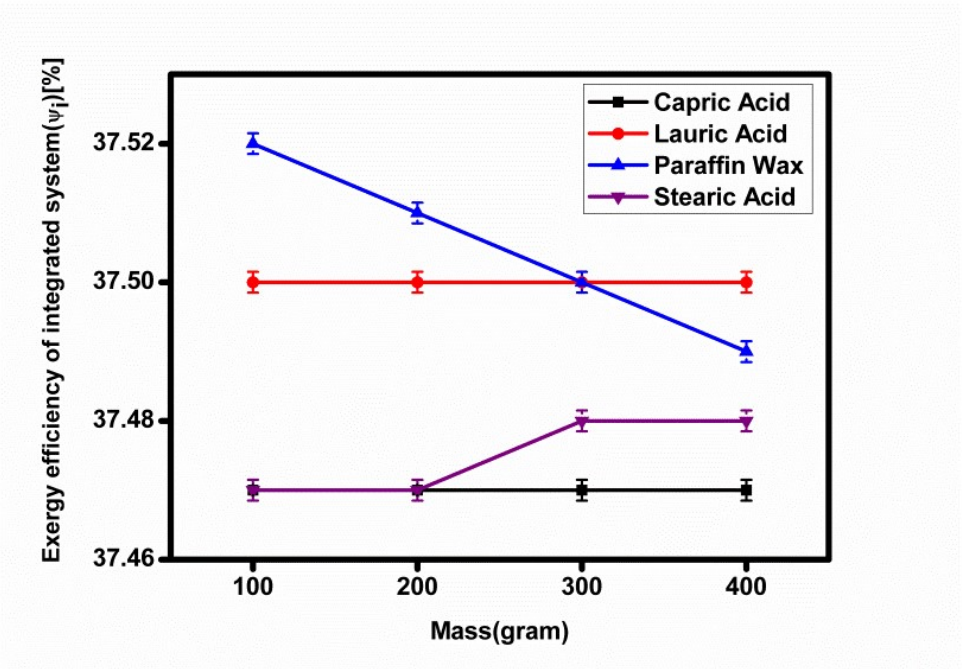

Fig.3.27. Variation in the exergy efficiency of the integrated system

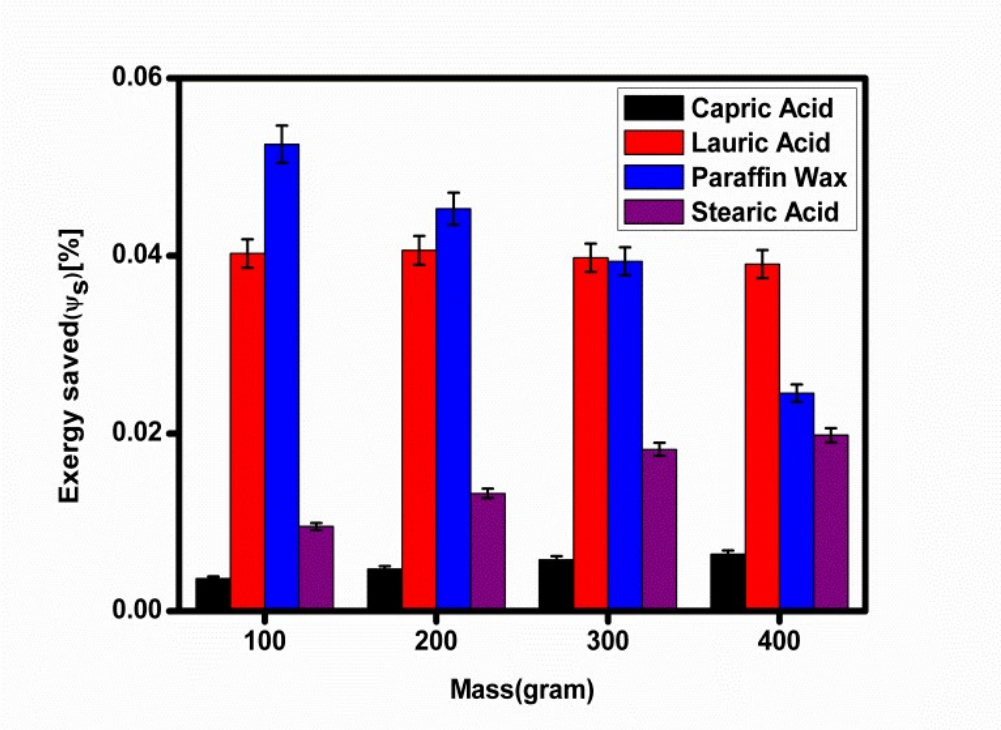

Fig.3.28. Variation in the exergy saved

The interpretation of exergy saved for the mass fraction variation of PCMs from 0.1kg to 0.4kg is shown in Fig. 3.28. It has been found that exergy savings of capric acid,

lauric acid, and stearic acid-based TES systems were increased by 74.5%, 2.96%, and 108.1%, respectively. However, with the mass fraction change of 0.1-0.4kg, the exergy saved was reduced by 39.55% in the paraffin wax PCM-based TES system. Exergy saved by lauric acid PCM at 0.3kg was higher than capric acid, paraffin wax, and stearic acid PCMs based on thermal energy storage integrated with engine exhaust due to better thermophysical properties less charging time, more excellent specific heat value, and slightly higher latent heat. Furthermore, the variation in error value for energy and exergy saved were obtained at 0.03-0.05% and 0.002-0.006%, respectively.

3.4.5. Validation of experimental results with theoretical estimations:

Due to measurement instrument errors and parameter uncertainties, experimental results have deviated from theoretical estimates. Table 3.7 shows the deviation of experimental results with theoretical estimations in case of energy and exergy analysis of CA, LA, PW, and SA PCMs based TES system:

Table 3.7: Validation of experimental parameters

S.No	**Parameters**	**Validation**
Energy Analysis of TES System		
1.	Energy of storage medium	**0.008-0.013 (kW)**
2.	The energy efficiency of charging	**0.1% - 0.4%**
3.	The energy efficiency of the integrated system	**0.1% - 0.2%**
4.	Energy saved	**0.15% - 0.24%**
Exergy Analysis of TES System		
5.	exergy of storage medium	**0.0001-0.0005(kW)**

6.	The exergy efficiency of charging	**0.01-0.04%**
7.	The exergy efficiency of the integrated system	**0.012-0.025%**
8.	exergy saved	**0.003-0.007%**

3.5. Highlights of the results:

The energy and exergy analysis of the thermal energy storage system with organic PCMs, i.e., capric acid, lauric acid, paraffin wax, and stearic acid PCMs integrated with engine exhaust, is performed. The following conclusions have been drawn from the experimental analysis for various mass fractions of organic PCM based thermal energy storage systems:

- The energy of the storage medium of capric acid, lauric acid, and stearic acid-based TES system has been increased by 122.8%, 5.66%, and 99.06%, respectively, as the mass fraction variation of PCMs from 0.1kg to 0.4kg.
- The energy saved in the paraffin wax PCM-based TES system was decreased by 53.19% for the mass fraction variation of 0.1-0.4kg.
- For the mass fraction variation of 0.1-0.4kg, the energy efficiency of the integrated system of capric acid, lauric acid, and stearic acid-based TES system increased by 0.23%, 0.076%, and 0.26%, respectively.
- The exergy efficiency of charging, capric acid, lauric acid, and stearic acid-based TES systems increased by 74.48%, 2.9%, and 108%, respectively, for the mass fraction variation of 0.1-0.4kg.

- The PCMs such as capric acid, lauric acid, and stearic acid-based TES systems, exergy saved 74.5%, 2.96%, and 108.1%, respectively. The exergy saved was reduced by 39.55% in the paraffin wax PCM-based TES system with a mass fraction change of 0.1-0.4kg.

The above analysis concludes that lauric acid PCM-based thermal energy storage can work at high temperatures and has better thermal energy storage performance at a 0.3kg mass fraction than capric acid, paraffin wax, and stearic acid PCMs. Thus, an organic PCMs-based thermal energy storage (TES) system has the more significant potential to store the energy as an option for a waste heat recovery system from the engine for green technology.

This page is intentionally left blank